Improvement of the Performance of DC/DC Converter Used for Transportations Applications. Test of Different Control Strategies

Alaa Hijazi, Eric Bideaux, Pascal Venet, Guy Clerc

Improvement of the performance of DC/DC converter used for transportations applications. Test of different control strategies

Alaa Hijazi, Eric Bideaux, Pascal Venet, Guy Clerc

Abstract— **This paper presents a DC/DC converter with supercapacitor stack for a trolleybus. After the description of transportation application, the performances of the system are studied by testing different control strategies. The comparison of SMC (Sliding mode Control) and PI controller on a developed test bench have shown the benefit of SMC in this type of application.**

***Index Terms*—Boost converter, PI controller, sliding mode, supercapacitor**

I. Introduction

DC to DC converters are more and more used in applications that required converting DC voltage from one level to another one.

Conventionally, PID controllers are used to control power converters [1] [2] [3]. However, these controllers, which are based on linearization techniques [4] [5], fails to perform satisfactory constrained specifications under large perturbation variations [6].

Sliding mode control (SMC) of power converters is an important alternative for controlling such systems, due to their capability to control nonlinear system and to provide robust stability and performance [4] [7] [8] [9].

The SMC has becoming an attractive subject in the field of the control of power electronic converters. The objectives of must research work are to simplify the design, to improve robustness, to reduce the number of components, and to prevent the chattering phenomena which is the origin of high frequency oscillations along the sliding surface.

The SMC for power converters is an old subject. Early works on the development of SMC for DC-DC Controllers appear in 1983 [10] [11] . This work shows the application of SMC to various topologies of second order DC-DC converters. A general method to synthesize SMC for most topologies of DC-DC converters is proposed in [12]. This study shows clearly the robustness of SMC toward load and parameters variation.

The study of several sliding surfaces has been conducted in [13], particularly surfaces that do not depend on the load current. Several studies ([12] [14] [15] [16] [17] [18]) have been interested with the problem of fixing the frequency of SMC. The solutions proposed consist of adding some triangular waveforms or adaptive hysteresis band to the sliding surface. Another works deals with eliminating the steady state error by adding an integral term in the sliding surface [19] [20].

However, despite being a popular research subject, SMC is still rarely applied in practical DC-DC converters [21]. So our goal in this paper is to explore the benefit of application of SMC in industrial application concerning the supply of trolleybus via supercapacitors stack associated with DC-DC converter.

The supply system of trolleybus consists of two parallel DC-DC converters (Fig. 1). The first converter (Trolleybus converter) regulates the voltage of the bus V_b to 330 Volts while the other one (Supercapacitors converter) manages the energy transfer between supercapacitors and trolleybus. When the voltage of trolleybus is more than 350 Volts, the supercapacitors will be charged. When the voltage decreases fewer than 310 Volts, the supercapacitors discharges to insure the continuity of the supply of the auxiliary of trolleybus (pump, air compressor, fans). The supercapacitors voltage must be always between 120 and 300 Volts. In this paper, we will focus on the discharge phase of supercapacitors. As the voltage of trolleybus is greater than the voltage of supercapacitors, our study is limited to the study of the control of boost converter.

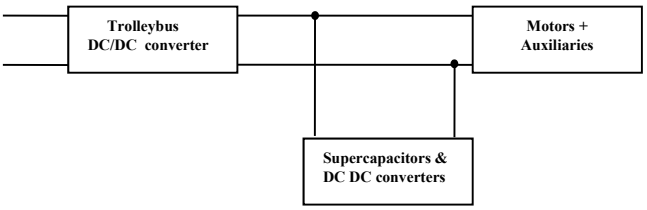

Figure 1 : Architecture of the trolleybus alimentation supply.

Due to its simplicity, boost converters are widely present in applications that need to increase voltage. However because of its non-minimum phase structure, the control of boost converter is more complicated than buck converter [22]. This paper deals with the application of sliding mode control to a boost converter, which is used for supplying a trolleybus with supercapacitors, during power micro-cuts. For many systems, in the trolley, such as electric air compressor, these cuts of electrical supply are very critical. Implementing an auxiliary energy source in the trolley improves the system reliability and decrease the energy consumption by recovering the braking energy. The electrical micro-cuts can take place during very short time, thus the importance of the dynamic performance of the controller.

In the second section, we present the theoretical study, concerning the synthesis of SMC and PI controller for boost converter. In the third section, the developed prototype is presented. Finally, the fourth section is dedicated to emphasize

the advantages and the drawbacks of the SMC by comparing the PI controller and the SMC structure performances.

II. THEORETICAL STUDY OF SMC AND PI CONTROLLER

A. *Mathematical model of a boost converter*

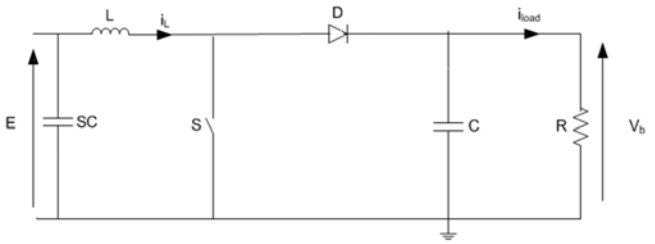

Figure 2 : Schematic of boost converter.

Fig. 2 shows the circuit of a boost converter. It consists of a DC input voltage E, which represents the voltage of the supercapacitors, the smoothing inductor L, the controlled switch S, the freewheeling diode D, the filter capacitor C and finally the load, which is modeled by the resistor R. Assuming that the circuit is in continuous conduction mode, which means that the inductors current never falls to zero, the mathematical model of boost converter can now be easily deduced by applying Kirchhoff's laws. The model of boost converter in continuous conduction mode is:

$$\begin{cases} C\dfrac{dV_b}{dt} = (1-u)i_L - i_{load}, \\ L\dfrac{di_L}{dt} = E - (1-u)V_b, \end{cases} \quad (1)$$

Where u is the switch state or the switch duty cycle in the case of average model, V_b and i_L are respectively the output voltage and the inductor current of the boost converter.

B. *Sliding mode controller for boost converter*

1) *Introduction*

The sliding mode control is a robust control, which is based on the concept of changing the controller in relation with the system state, in order to obtain the desired response. The sliding mode control is a bang-bang controller that switches abruptly between two states. The idea is to divide the state space by a boundary called sliding surface, which defines two subspaces corresponding to two possible states of the controller. Stabilization on the sliding surface is obtained by switching S each time a boundary decision trajectory is crossed. In order to have a stable equilibrium point, three conditions must be satisfied (figure 3): attractiveness condition, sliding condition and stability condition.

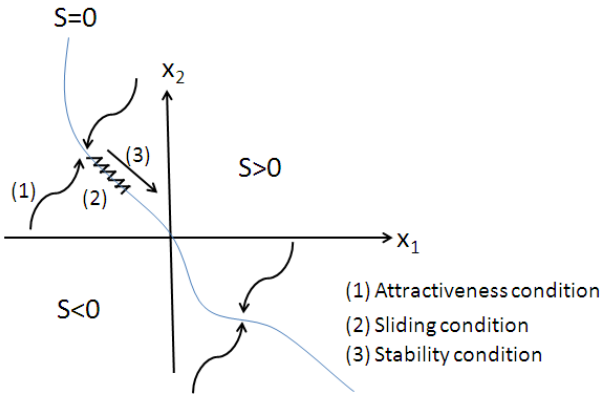

Figure 3 : Sliding mode condition.

The control should aim to make the surface attractive. Regardless the position of the system in state space, the control should insure that the system moves toward the surface (attractiveness). Once the surface is reached, we must ensure that the system slides over the surface (sliding condition). Finally, we should verify that the equilibrium point is stable, so the system goes toward the equilibrium point (stable condition).

For boost converter, we choose the sliding surface as a linear combination of the state variables (i_L,V_b) :

$$S = K_1(V_b - V_{ref}) + K_2(i_L - I_{ref}) \quad (2)$$

Where V_{ref} and I_{ref} are the output voltage and inductor current reference, K_1 and K_2 constants $\in R^+$.
The reference current I_{ref} depends on the operating point, so that :

$$I_{ref} = \frac{V_{ref} i_{load}}{E} \quad (3)$$

where $i_{load} = \frac{V_b}{R}$.

The reference current is dynamic and it tends toward I_{ref}^{eq} corresponding to the equilibrium state (V_{ref}, I_{ref}^{eq}).
Replacing I_{ref} by its value from (3) in the expression of the commutation surface (2), we obtain:

$$\begin{aligned} S &= K_1(V_b - V_{ref}) + K_2 i_{load} - \frac{K_2 V_{ref} V_b}{R.E} \\ &= (K_1 - \frac{K_2 V_{ref}}{R.E})(V_b) + K_2 i_L - K_1 V_{ref} \end{aligned} \quad (4)$$

Writing this last equation in a new coordinate system ($x_1 = V_b - V_{ref}, x_2 = i_L - I_{ref}^{eq}$), we have:

$$S = K_1' x_1 + K_2 x_2 \quad (5)$$

In SMC, we usually determine u as following:

$$u = \begin{cases} 1 \text{ if } S < -\Delta \\ \\ 0 \text{ if } S > \Delta \end{cases}$$

Where S is the sliding surface. Δ is an hysteresis band added to limit the switching frequency.

2) Calculation of system parameters

Referring to the work presented in [23] , to insure the stability of equilibrium point the gain of controller must respect this condition:

$$\frac{K_1}{K_2} < \frac{RCE}{V_{ref}L} + \frac{V_{ref}}{RE} \tag{6}$$

The inequality (6) provides general information about region where stability of the system is insured. However, the choice of these parameters has a great influence on the performance of the system and especially when the system presents large variation around operating point.

Let us write the model of boost converter (1) in the state space (x_1, x_2) where the equilibrium point (V_{ref}, I_{ref}^{eq}) is the origin. We obtain:

$$\begin{cases} C\dfrac{dx_1}{dt} = (1-u)\left(x_2 + I_{ref}^{eq}\right) - \left(\dfrac{x_1 + V_{ref}}{R}\right), \\ \\ L\dfrac{dx_2}{dt} = E - (1-u)(x_1 + V_{ref}), \end{cases} \tag{7}$$

The existence condition of sliding mode implies that both S and $\dot{S}$ will tend to zero when t tend to infinity. The existence condition of the sliding mode is deduced by taking $\left(V = \frac{1}{2}S^2\right)$ as a Lyapunov function and by proving then that $S\dot{S} < 0$ (when $S \to 0$), the fulfillment of this inequality ensures the existence of sliding mode around the commutation surface.

By calculating $S\dot{S}$ to be negative for u=0 and 1, we can deduce that the sliding region is limited by the following inequalities:

$$\begin{cases} x_1\left[\dfrac{-K_1'}{RC} - \dfrac{K_2}{L}\right] + \dfrac{x_2 K_1'}{C} + \\ K_2\left[\dfrac{E}{L} - \dfrac{V_{ref}}{L}\right] - K_1'\left[\dfrac{V_{ref}}{RC} - \dfrac{I_{ref}^{eq}}{C}\right] < 0 \\ \\ -\dfrac{K_1' x_1}{RC} + \dfrac{K_2 E}{L} - \dfrac{V_{ref} K_1'}{RC} > 0 \end{cases} \tag{8}$$

Depending on whether or not the system intercepts the sliding surface in the sliding zone, the dynamic performance of the system can be affected as we can see from the figure 4.

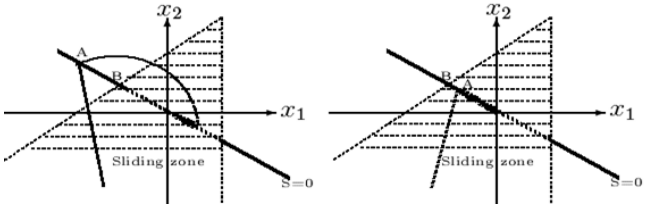

Figure 4 : Sliding mode with (a) and without overshoot (b).

Let $A(x_{1A}, x_{2A})$ be the intersection of the system dynamics with the commutation surface and $B(x_{1B}, x_{2B})$ the limit of sliding part as shown in (Fig. 4). Supposing that at $t = 0$ the output voltage is equal V_{ini} and the current in the inductor is zero. As at $t = 0$ the surface S will be negative, then $u = 1$ and we obtain:

$$\begin{cases} C\dfrac{dx_1}{dt} = -\left(\dfrac{x_1 + V_{ref}^e}{R}\right), \\ \\ L\dfrac{dx_2}{dt} = E. \end{cases} \tag{9}$$

By solving these two equalities taking into account initial conditions, we obtain:

$$x_1 = V_{ini} e^{-\frac{L(x_2 + I_{ref}^e)}{RCE}} - V_{ref}^e . \tag{10}$$

This equation represents the dynamic of the system before intercepting the surface at the point A. From $S = 0$ and from (10) we deduce the coordinate of point A:

$$x_{2A} = \frac{K_1'}{K_2}\left(-V_{ini} e^{-\frac{L(x_{2A} + I_{ref}^e)}{RCE}} + V_{ref}^e\right). \tag{11}$$

Solving this last equation we can obtain x_{2A} function of the parameters of the converter and controller.

From the equation of the commutation surface and the limit of sliding zone defined by (8), we deduce the coordinate of point B, we have:

$$x_{2B} = \frac{K_1'}{K_2} \frac{\dfrac{K_1'\left(\dfrac{V_{ref}^e}{RC} - \dfrac{I_{ref}^e}{C}\right)}{K_2} - \left(\dfrac{E}{L} - \dfrac{V_{ref}^e}{L}\right)}{\dfrac{1}{C}\left(\dfrac{K_1'}{K_2}\right)^2 + \dfrac{K_1'}{K_2 RC} + \dfrac{1}{L}}. \tag{12}$$

We can now deduce that the system intercepts the commutation surface in the right part if the controller parameters are selected in such a way that:

$$\|OA\| < \|OB\|. \tag{13}$$

On the other side, the theoretical approach of sliding control makes the assumption that the hysteresis band is null and by consequence the frequency is infinite which is not practically possible due to the characteristic and limitation of circuit components.

In addition to the hysteresis band Δ, the gains of controller

have great influence on the operating frequency.

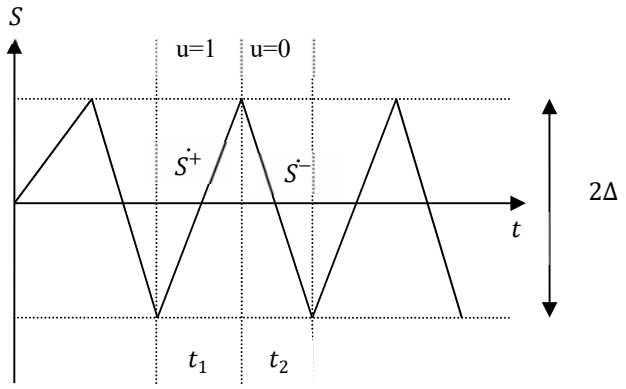

Figure 5 : Sliding regime with hysteresis band.

Based on the state of the switch and looking to figure 5, we can deduce the rise time "t_1" and fall time "t_2" :

$$t_1 = \frac{2\Delta}{\dot{S}^+} \tag{14}$$

$$t_2 = \frac{2\Delta}{\dot{S}^-} \tag{15}$$

From these equations and the expression of sliding surface (5), we can deduce the expression of the hysteresis band function of the controller and circuit parameters:

$$\Delta = \frac{1}{2f}\left(\frac{1}{A+B}\right) \tag{16}$$

Where A and B are equal to:

$$A = \frac{1}{\frac{K_2}{L}E - \frac{V_{ref}^e K_1'}{RC}} \tag{17}$$

$$B = \frac{1}{K_1'\left(\frac{(V_{ref}^e)^2}{REC} - \frac{V_{ref}^e}{RC}\right) + K_2\left(\frac{E}{L} - \frac{V_{ref}^e}{L}\right)} \tag{18}$$

C. PI controller for boost converter

As in the case of SMC, we choose in this paragraph to synthesize a PI control of boost converter by means of two loops (current and voltage loop). This improves dynamic performance and robustness of the system. In fact, the presence of a right hand plan zero (RHPZ) in the transfer function of the boost make its control by a single voltage loop inadequate and complicated in some cases [24] [5]. The structure of the control is shown in figure 6. The corrected error between the reference voltage and the measured voltage serves as a reference for the inner current loop which generates the duty cycle for the converter.

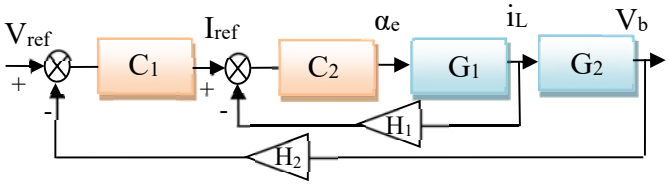

Figure 6 : two loop control structure

C_1 and C_2 are respectively the controllers for outer and inner loop. G_1 and G_2 are respectively the transfer function for outer and inner loop. H_1 and H_2 are respectively the gain of current and voltage sensor.

The transfer function G_1 and G_2 are obtained from linearization of the converter model (1) around an equilibrium point (α_e, R). To obtain the transfer function G_1 and G_2, we refer to the works presented in [25]. We have:

$$G_1(s) = \frac{\hat{I}_L(s)}{\widehat{\alpha_e}(s)} = \frac{2V_b}{R(1-\alpha_e)^2}\frac{1+\frac{RC}{2}s}{1+\frac{L}{R(1-\alpha_e)^2}s+\frac{LC}{(1-\alpha_e)^2}s^2} \tag{19}$$

$$G_2(s) = \frac{\hat{V}_b(s)}{\hat{I}_L(s)} = \frac{(1-\alpha_e)R}{2}\frac{\left(1-\frac{L}{R(1-\alpha_e)^2}s\right)}{1+\frac{RC}{2}s} \tag{20}$$

The terms $\hat{x}$ correspond to small variation of the term x. α_e is the duty cycle.

The analysis of transfer functions shows the presence of a zero in the right part of the complex plane, the pulsation of this zero is equal to:

$$\omega_z = \frac{R(1-\alpha_e)^2}{L} \tag{21}$$

This unstable zero is present in all the converters that indirectly store the energy. These converters first store the energy in the inductor, then returns it to the load. If the dynamics of the change of duty ratio compared to a disturbance is very fast, naturally the inductor limits the current rise. So the current in the inductor will not be able to increase at the same speed as the duty cycle. This automatically leads to a voltage drop and therefore to oscillations.

The zero adds a phase shift of 90 ° to the transfer function. If the zero appears close to the cutoff frequency, it has a negative effect on the phase margin of the system by reducing this latter, which affects the stability and causes the system to

oscillate. To overcome this problem, we should limit the dynamic variation of the duty cycle. As it's shown in [26], the bandwidth of the system must be limited to 30 % of the RHP (Right Half Plane) zero pulsation.

III. PROTOTYPE MODEL

To compare SMC and PI controller, we have developed a test bench, which consists of a DC power supply feeding a resistive load and a reversible converter that manages the energy stored in 8 supercapacitors connected in series (figure 7). This configuration allows maintaining the DC bus voltage constant, in case of load variation or electrical cuts of DC power supply. This test bench is therefore close to the structure of the power system of the trolleybus, where we have two type of alimentation: the primary source from the catenaries and the secondary one from supercapacitors. Control of the converter is done through a DSPACE 1104 card. The connection between the converter and the card is done via optic fiber. The voltage and current of the supercapacitor and the load has been measured. The currents are measured with a LEM current sensor. The voltages are measured based on a voltage divider, associated with an isolated amplifier.

The measured current and voltage are connected to the ADC inputs of the DSPACE system and scaled to 0-5 V. A simple hysteresis control is adopted for buck converter.

The parameter of the converters is summarized in table 1.

Table 1 : Converter's parameters.

Parameter name	Symbol	Value
Input voltage	E	10-20 V
Output voltage	V_b	40 V
Capacitor	C	1600 µF
Inductor	L	160 µH
Load resistance	R	5-20 Ω

IV. RESULTS AND DISCUSSION

In the case of SMC, both the controller's gain and the hysteresis band are chosen to obtain switching frequency above 5 kHz and a good dynamic performance.

The synthesis of PI correctors must be around the critical point in terms of stability, which corresponds in the case of boost converter to the minimum input voltage and maximum load.

The correctors have been designed to obtain:

- A response time for the inner loop about 1.5 ms
- A phase margin for external loop 60 ° and a cutoff frequency of about 30 % of the pulsation of RHPZ (to avoid the adverse effect of the RHPZ).

We have utilized the toolbox Sisotool from Matlab@Mathworks in order to synthesize the controllers and we obtain:

$$C_1(s) = 822.01\frac{1 + 0.0025\text{s}}{\text{s}} \quad (22)$$

$$C_2(s) = 165.05\frac{1 + 0.00048s}{s} \quad (23)$$

The open loop diagram of the voltage loop is presented in the figure 8.

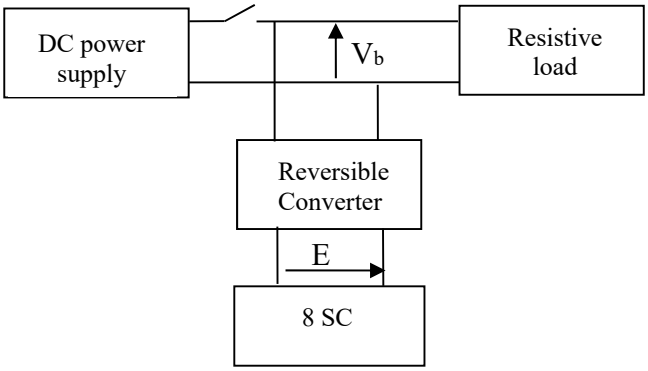

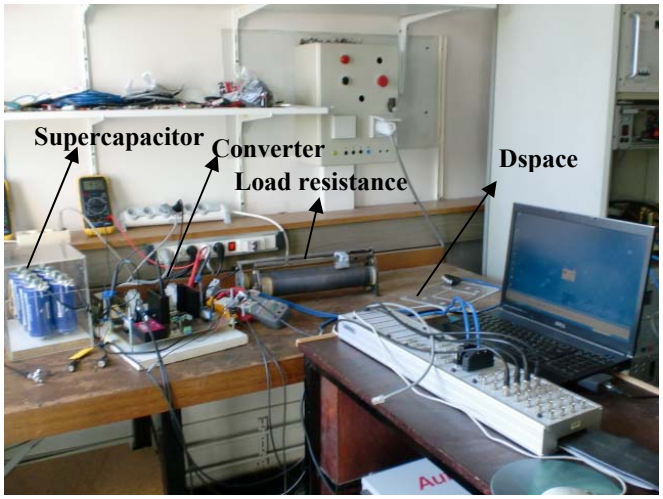

Figure 7 : experimental prototype.

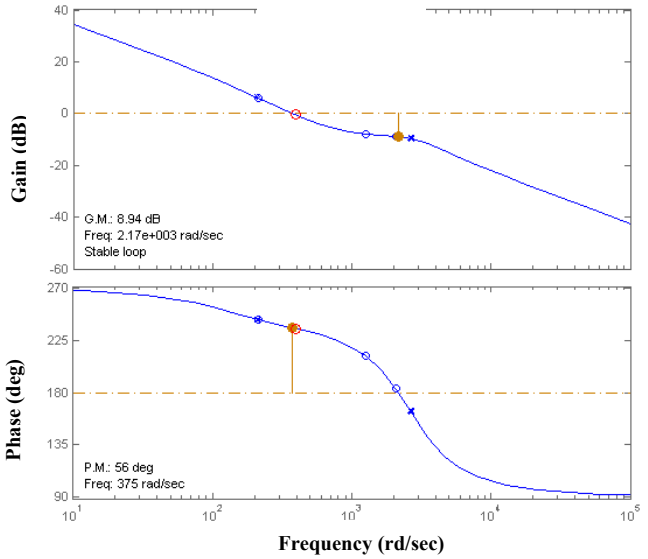

Figure 8: Bode diagram of the voltage loop.

The switch control of SMC is done from the digital output of the DSPACE using TTL voltage level.

In order to compare the performances of the controllers, we have realized a series of test that simulate the variation of the load or a DC power supply interruption. In this case, the supercapacitors provide electrical power to the load via the boost converter. The reference voltage for V_b in this case is equal to 40 V. Several test campaigns were made in order to compare the control laws in different conditions. The first one consists of varying the load from 20 to 5 Ω. The results obtained for two voltage levels are shown figure 9 and 10. We can notice the excellent dynamic performance of SMC compared to PI controller. The SMC allows the system to reach the reference voltage, very quickly (between 0.1 and 0.5 ms) without oscillations. With the PI controller, the bus voltage reference is reached more slowly (between 7 and 10 ms). This implies a voltage drop of several volts.
We can also remark the non-linear aspect of SMC. Its performance is not influenced by a change of the operating point. However, control by sliding mode has two drawbacks: the static error and the variable switching frequency of the converter. In fact, a maximum static error of 2% was observed for a voltage across the supercapacitors equal to 10 V (V_b equal 39.2 instead of 40 V). Increasing the order of the controller by adding an integrator can cancel this error. The switching frequency varies between 4.5 and 14 kHz.

After having tested the performance of controllers in different conditions characterizing the load variations, we illustrate in second test campaign, the performances of the controllers, in the case of loss of the alimentation. These tests have the advantage to illustrate the performance of controllers, based on an initial state far from the equilibrium point. We can remark that the power supply voltage is 43 V and the objective of the controllers is to regulate the output DC voltage to 40 V when the output voltage decreases below this limit. The results are shown in figure 11 and 12. The results show the excellent dynamic performance of SMC. The bus voltage has stabilized after 1 ms without overshoot in the case of SMC. The PI controller needs 10 ms to reach the same voltage.

Table 2 and 3 summarizes the conclusions obtained concerning the controller comparison.

Table 2 : Summary of the comparison between SMC and PI.

	PI	SMC
Rapidity	-	+
Robustness	-	+
Non linearity	-	+
Static error	+	-
Constant frequency	+	-

Table 3 : Comparison between the performance of SMC and PI.

	PI	SMC
Maximum response time	16 ms	1 ms
Maximum Steady state error	No error	2 %
Maximum Amplitude of oscillation	10 V	No oscillation
Switching Frequency variation	No variation	Between 5 and 14 kHz

V. CONCLUSION

In this paper, the comparison between SMC and PI control has been realized for a boost converter used in supercapacitors stack for transportation applications. A test bench have been developed and presented. The different tests have shown clearly the advantage of SMC toward a classical PI controller. The results show that the SMC allows having a fast response with no oscillation. In other side, it has been shown that the boost converter controlled by SMC is penalized by the steady state error and the variation of switching frequency. These drawbacks can be resolved by introducing an integral term in the sliding surface and by adapting the hysteresis band with the operating point.

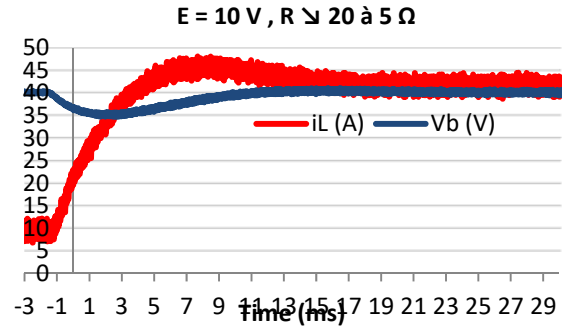

(a)

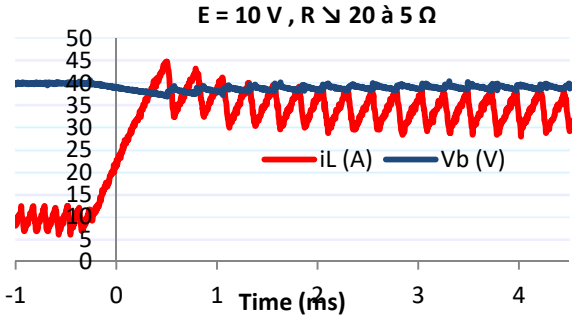

(b)

Figure 9 : Experimental results for a variation of load from 20 to 5 Ω and for a supercapacitors voltage equal to 10 V (a : PI, b : SMC).

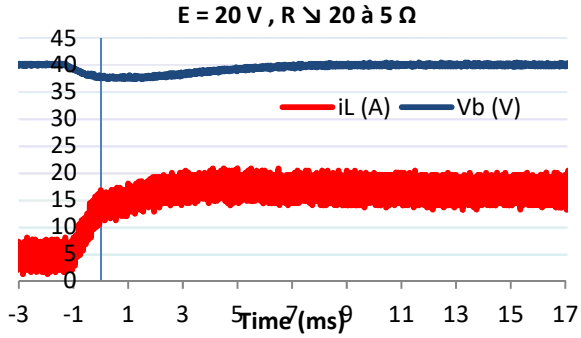

(a)

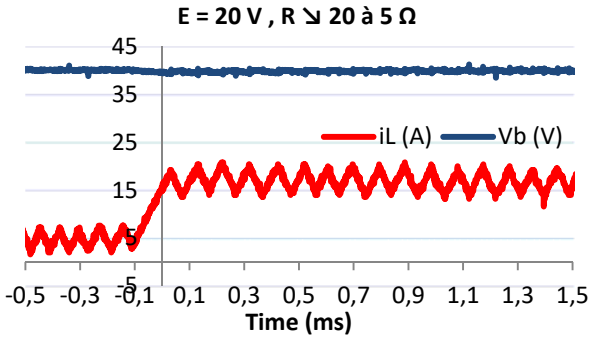

(b)

Figure 10 : Experimental results for a variation of load from 20 to 5 Ω and for a supercapacitors voltage equal to 20 V (a : PI, b : SMC).

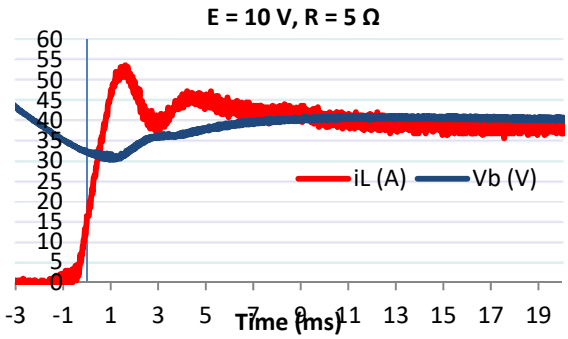

(a)

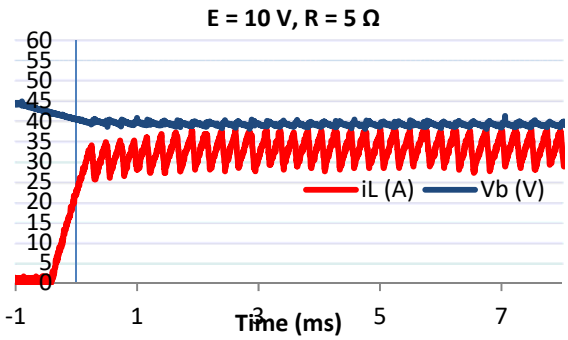

(b)

Figure 11: Experimental results for power supply cut with a supercapacitors voltage equal to 10 V (a : PI, b : SMC).

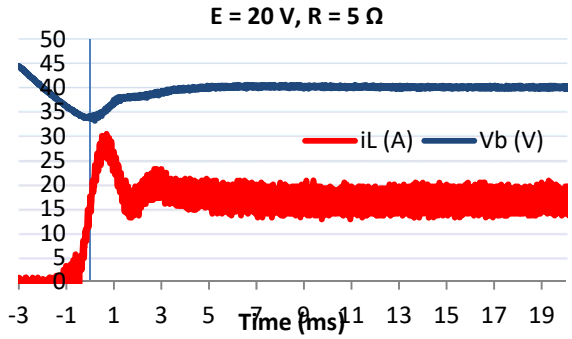

(a)

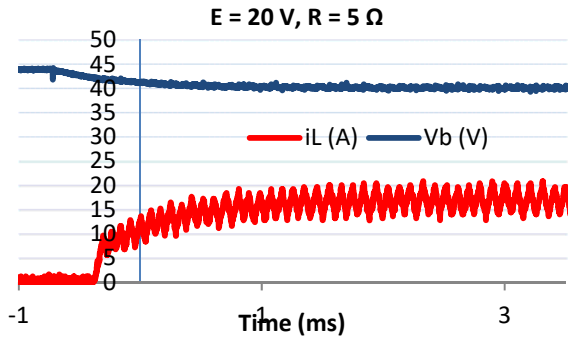

(b)

Figure 12 : Experimental results for power supply cut with a supercapacitors voltage equal to 20 V (a : PI, b : SMC).

VI. References

[1] S. Arulselbi, G. Uma et M. Chidambaram, «Design of PID controller for boost converter with RHp zero,» chez *IPEMC*, China, 2004.

[2] L. Guo, J. Hung et R. Nelms, «Design and implementation of a digital PID controller for a buck converter,» chez *36th Intersociety Energy Conversion Engineering Conference*, Savannah, Georgia, 2001.

[3] H. Mingzhi et X. Jianping, «Nonlinear PID in digital controlled buch converters,» chez *APEC*, Anahein , 2007.

[4] M. Rashid, Power electronics handboos, Academic press , 2001.

[5] A. Forsyth. et S. Mollov., «Modelling and control of DC-DC converters,» *Power Engineering Journal,* vol. 12, n° %15, 1998.

[6] V. Racirah et P. Sen, «Comparative Study Of Proportional-Integral Sliding Mode, and Fuzzy Logic Controllers for Power Converters,» *IEEE Transactions On Industry Applications,* vol. 33, n° %12, pp. 518-524, 1997.

[7] V. Utkin, Sliding mode control and optimization, Springer-Verlag, Éd., 1992.

[8] V. Utkin, «Variable structure systems with sliding modes,» *IEEE Transaction On Automatic Control,* vol. 12, n° %15, pp. 212-222, 1977.

[9] L. S. R. T. P. Malesani, «Performance optimization of Cuk converters by sliding-mode control,» *IEEE Transactions on Power Electronics,* vol. 10, n° %13, pp. 302 - 309, 1995.

[10] F. Bilalovic, O. Muasic et A. Sabanovic, «Buck converter regulator operating in the sliding mode,» chez *International Conference on Power Conversion*, Geneva, 1983.

[11] R. Venkataramanan, A. Sabanovic et S. Cuk, «Sliding mode control of DC-to-DC converters,» chez *IEEE Conference on Industrial Electronics, Control and Instrumentations*, California, 1985.

[12] P. Mattavelli, L. Rossetto, G. Spiazzi et P. Tenti, «General-purpose sliding-mode controller for DC/DC converter applications,» chez *IEEE Power Electronics Specialists Conference Record*, seatle, 1993.

[13] D. Cortes et J. Alvarez, «Robust sliding mode control for the boost converter,» chez *Proceedings of VIII IEEE International Power Electronics Congress*, Toulouse, 2002.

[14] B. Cardoso, A. Moreira, B. Menezes et P. Cortizo, «Analysis of switching frequency reduction methods applied to sliding mode controlled DC-DC converters,» chez *IEEE Applied Power Electronics Conference and Exposition*, Boston, 1992.

[15] L. Iannelli et F. Vasca, «Dithering for sliding mode control of DC/DC converters,» chez *IEEE Power Electronics Specialists Conference Record*, Aachen, 2004.

[16] S. Tan, Y. Lai, C. K. Tse et M. Cheung, «Adaptive feedforward and feedback control schemes for sliding mode controlled power converters,» *IEEE Transaction on power electronics,* vol. 21, n° %11, pp. 182-192, Jan 2006.

[17] M. Bekemans et D. Sigismondi, «Reglage par mode de glissement synchronisé par PLL,Application à un convertisseur DC/DC de type buck,» *Revue scientifique des instituts superieurs industrieles,* n° %120, p. 197, 2006.

[18] Y. M. L. C. K. T. I. M. K. H. C. Siew-Chong Tan, «A Fixed-Frequency Pulsewidth Modulation Based Quasi-Sliding-Mode Controller for Buck Converters,» *IEEE Transaction on Power Electronics,* vol. 20, n° %16, 2005.

[19] H. Maker, H. Gualous et R. Outbib, «Sliding Mode Control with Integral of Boost Converter by microcontroller,» chez *IEEE Joint CCA, ISIC and CACSD 2006*, Munich,, 2006.

[20] S.-C. Tan, Y. Lai et C. Tse, «Indirect Sliding Mode Control of Power Converters Via Double Integral Sliding Surface,» *IEEE Transactions on Power Electronics,* vol. 23, n° %12, pp. 600 - 611 , 2008.

[21] Y. L. C. K. Siw-Chong Tan, «General Design Issues of Sliding-Mode Controllers in DC-DC converters,» *IEEE transactions On Industrial Electronics,* vol. 55, n° %13, March 2008.

[22] S. Kapat, A. Patra et S. Banerjee, «A Current-Controlled Tristate Boost Converter With Improved Performance Through RHP Zero Elimination,» *IEEE transactions on power electronics,* vol. 24, n° %13, pp. 776-786, March 2009 .

[23] A. Hijazi, M. Di loreto, E. Bideaux, P. Venet, G. Clerc et G. Rojat, «Sliding mode control of boost converter: Application to energy storage system via supercapacitors,» chez *EPE*, Barcelone, 2009.

[24] M. Mitchell, «Tricks of the Trade: Understanding the Right-Half-Plane Zero in Small-Signal DC-DC Converter Models,» *IEEE Power Electronics Society NEWSLETTER,* n° %11, 2001.

[25] F. F. J.P. Ferrieux, Alimentations à découpage convertisseurs à résonance, 3e edition éd., Dunod, 1999.

[26] C. Bassot, Switch-Mode Power Supply: Spice Simulations and Practical Designs, McGraw-Hill, 2008.